Single-crystal and powder neutron diffraction experiments on $FePS_3$: Search for the magnetic structure

K. C. Rule,[1,*] G. J. McIntyre,[2] S. J. Kennedy,[3] and T. J. Hicks[1]
[1]*School of Physics, Monash University, Clayton 3800, Australia*
[2]*Institut Laue-Langevin, Boîte Postale 156, 38042 Grenoble Cedex 9, France*
[3]*Bragg Institute, Australian Nuclear Science and Technology Organisation, Menai, New South Wales 2234, Australia*
(Received 9 July 2007; published 5 October 2007)

The long-accepted magnetic structure of $FePS_3$ has recently been refuted through extensive powder neutron diffraction studies. Single-crystal neutron diffraction, using both quasi-Laue and monochromatic techniques, has now been conducted to reveal more information about the nature of the magnetic ordering in this compound. The magnetic unit cell was found to be twice as large as the crystallographic cell in both the a and b directions and around three times as large along the c direction, giving a propagation vector of $[\frac{1}{2}\ \frac{1}{2}\ 0.34]$. There is incomplete long-range magnetic order along the c^* direction due to weak Fe-Fe interactions and large anisotropy in that direction. The variation of the spontaneous moment with temperature closely resembles that for an antiferromagnetic two-dimensional Ising model on a honeycomb lattice.

DOI: 10.1103/PhysRevB.76.134402 PACS number(s): 75.25.+z, 75.50.Ee, 75.30.Gw, 75.40.−s

I. INTRODUCTION

Iron thiophosphate is a good example of a quasi-two-dimensional (2D) antiferromagnetic material. Along with other members of the thiophosphate family, $FePS_3$ has been of interest since the late 1960s due to its low-dimensional crystal structure.[1] As a consequence of this layered structure, $FePS_3$ also shows quasi-2D magnetic characteristics.[2] The magnetic Fe layers are spatially separated by large nonmagnetic gaps which reduce the strength of the magnetic interactions perpendicular to the layers. These materials are relatively simple to synthesize in a laboratory, forming monoclinic single crystals with a structural space group of $C2/m$ and with $a \approx 5.93$ Å, $b \approx 10.28$ Å, $c \approx 6.72$ Å, and $\beta \approx 107.1°$.[1] The crystal structure of this family of compounds can be seen in Fig. 1(a). The transition metal ions form a honeycomb structure within the ab plane, which is flanked by phosphorous dumbbells. The bond between the P-P pairs parallel to the c axis is 2.2 Å.[3] Two layers of sulfur atoms, which are in turn separated by van der Waals gaps, separate each Fe-P layer. Both the crystal and magnetic interactions are weaker along the third dimension, perpendicular to the ab plane, which has previously made this an interesting material for intercalation investigations.[4,5]

The magnetic structure of $FePS_3$ has been derived and accepted for over 20 years; however, our recent neutron studies have found this structure to be incorrect.[7] The magnetic structure initially proposed by Le Flem *et al.*[6] had collinear moments aligned perpendicular to the ab plane [Fig. 1(b)]. Within the plane, the moments were arranged in ferromagnetic chains, which are coupled antiferromagnetically. The planes were also coupled antiferromagnetically along the z direction. Kurosawa *et al.*[8] performed neutron diffraction experiments on a stack of single crystals of $FePS_3$ aligned along [0 0 1] and claimed that their results supported the structure of Le Flem *et al.*; however, the published structure of the Kurosawa *et al.*, shown in Fig. 1(c), is subtly different to that shown in Fig. 1(b). The ferromagnetic chains of Fe are rotated by 60° in the ab plane from those in the structure of Le Flem *et al.*

Recently, some of us[7] have revealed large inconsistencies in the paper by Kurosawa *et al.*[8] Their tabulated neutron diffraction data do not support the conclusions within the body of the article. In particular, their definition of the magnetic structure of $FePS_3$, which has been widely accepted for many years, does not correspond to their observations. It is

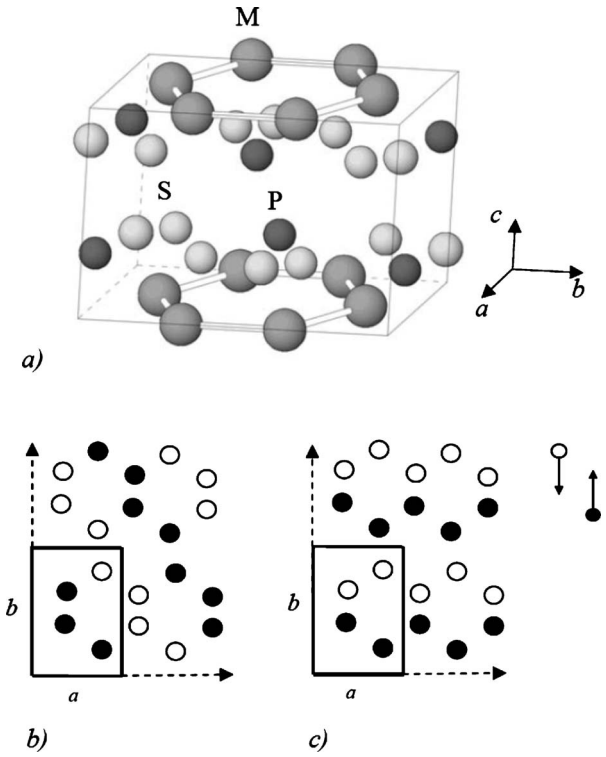

FIG. 1. (a) Crystallographic structure of MPS_3 (M = Mn, Fe, Ni). (b) and (c) show two different proposed magnetic structures of $FePS_3$ in the ab plane; (b) was proposed by Le Flem *et al.* (Refs. 1 and 6) while (c) shows structure described by Kurosawa *et al.* (Ref. 8). The solid square represents a single structural unit cell and the arrows represent the magnetic moment directions parallel to c^*.

 ©2007 The American Physical Society

clear that the propagation vector of $[0\ 0\ \frac{1}{2}]$ could not appropriately describe the neutron diffraction data. The two lowest-angle magnetic reflections $(0\ 1\ \frac{1}{2})$ and $(0\ 1\ \frac{3}{2})$ associated with the nuclear reflections (0 1 1) and (0 1 2) by addition of this propagation vector are not observed. It appears as though the propagation vector of $[0\ 0\ \frac{1}{2}]$ was chosen because it allows for a magnetic cell double the nuclear unit cell along the *c* direction. In the recent investigation by Rule *et al.*,[7] the powder neutron diffraction patterns displayed magnetic peaks at much lower scattering angles than reported by Kurosawa *et al.* The propagation vector of $k=[0\ 0\ \frac{1}{2}]$ was unable to describe these additional magnetic peaks which are located between 0.5 and 0.8 $Å^{-1}$ in Q. A new magnetic structure and propagation vector were, however, not immediately evident from the powder diffraction data, due mainly to the diffuseness of these magnetic peaks. Time-of-flight measurements taken with polarized neutrons indicated that these peaks were indeed elastic within an energy resolution of 200 μeV.[9] Thus the diffuse band was considered to contain unresolved magnetic Bragg peaks rather than energy-dependent events such as magnons. The current research focuses on a closer investigation of the magnetic reflections of $FePS_3$ using two different, complementary neutron diffraction techniques, which utilize a single-crystal sample. The aim was to find and index magnetic peaks to determine unambiguously the propagation vector. From this, models of the magnetic structure of $FePS_3$ are proposed.

II. EXPERIMENTAL DETAILS

Stoichiometric quantities of high-purity base elements were combined in an evacuated quartz tube and placed in a horizontal furnace. The quartz tube was heated with a gradient of 690–630 °C with crystal nucleation occurring at the cooler end after two weeks. The crystals formed as thin platelets with maximum dimensions of about $10\times10\times0.1$ mm^3.

A large, well-formed crystal was chosen for the single-crystal experiments conducted at the Institut Laue-Langevin (ILL) in France. The sample was mounted on a pinlike sample holder and placed within a He-flow cryostat. This was mounted on the Laue neutron diffractometer, very-intense vertical-axis laue diffractometer (VIVALDI), at the ILL.[10,11] VIVALDI uses a polychromatic neutron beam with wavelengths between 0.8 and 5.2 Å, and its cylindrical image-plate detector subtends more than 2π sr at the sample to permit rapid and extensive surveys of reciprocal space. Laue patterns were recorded at both 5 and 140 K for a variety of sample orientations. The temperatures were chosen such that 5 K was sufficiently below the magnetic ordering temperature, $T_N=120$ K, to ensure maximum magnetic ordering and peak intensities. 140 K was chosen to be sufficiently greater than T_N such that the sample was not magnetically ordered. The data from VIVALDI were analyzed with the program LAUEGEN, which matched diffraction patterns for the monoclinic space group $C2/m$ with the observed nuclear peaks.[12]

Magnetic reflections could be identified in the Laue patterns, but indexing was difficult due to their small number and to their diffuseness (*vide infra*). The opportunity arose to collect limited complementary data on the monochromatic four-circle single-crystal diffractometer, D19, also at the ILL.[13] For this experiment D19 was equipped with a $4°\times64°$ vertically curved position-sensitive detector, which also allowed reasonably extensive sampling of reciprocal space in three dimensions, although unlike in the Laue technique rotation of the sample was still necessary. The sample was retained on the same pin for the D19 measurements, but was mounted in a cryorefrigerator. The wavelength of the incident neutron beam was set to the nominal value of 1.5469 Å from a Cu (2 0 0) monochromator for the duration of the experiment. Since the same sample mount was used in both experiments, the indexing of the nuclear reflections from VIVALDI could be readily transferred to the reflections observed on D19. The sample was then cooled to 20 K, the minimum available using the D19 cryorefrigerator. A limited number of scans were made at 20 K, at 100 K, and one scan was repeated in small temperature steps from 20 to 140 K.

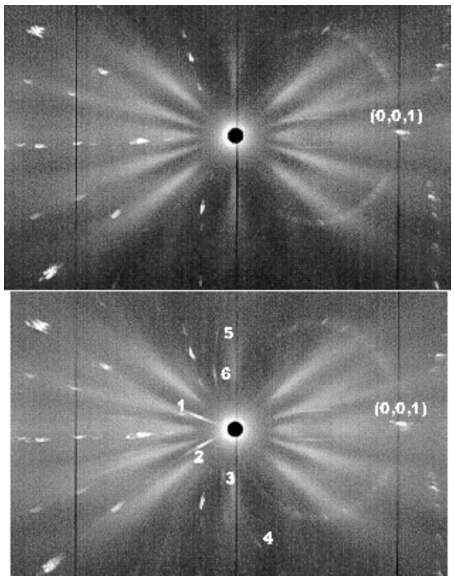

FIG. 2. Laue neutron diffraction patterns from VIVALDI at a single sample orientation. The pattern in the upper panel was taken at 140 K, showing only nuclear diffraction. The pattern in the lower panel was taken at 5 K, in the magnetically ordered state.

III. EXPERIMENTAL RESULTS

A typical VIVALDI Laue pattern for a single sample orientation can be seen in Fig. 2. The pattern in the upper panel was recorded at 140 K, while the pattern taken at 5 K can be seen in the lower panel. The black spot in the center of each pattern is the exit hole for the transmitted neutron beam. The dull extended streaks radiating from the center are due to scattering from the polycrystalline aluminum heat shields of the cryostat. Additional extended reflections near the transmitted beam are evident in the 5 K pattern, and are attributed to magnetic ordering. The most prominent magnetic reflections have been numbered 1–6.

Indexing of the 140 K VIVALDI patterns using

TABLE I. VIVALDI magnetic peak classification for peaks numbered 1–6 in Fig. 3.

Peak No.	1	2	3	4	5	6
Crystallite A	$\frac{1}{2}\ \frac{1}{2}\ \frac{1}{3}$			$\frac{3}{2}\ \frac{5}{2}\ \frac{1}{3}$	$\frac{3}{2}\ \frac{1}{2}\ \frac{2}{3}$	$\frac{3}{2}\ \frac{1}{2}\ \frac{1}{3}$
Crystallite B	$\frac{1}{2}\ \frac{1}{2}\ \frac{1}{3}$	$\frac{1}{2}\ \frac{1}{2}\ \frac{1}{3}$	$\frac{1}{2}\ \frac{5}{2}\ \frac{1}{3}$	$\frac{1}{2}\ \frac{7}{2}\ \frac{1}{3}$	$\frac{1}{2}\ \frac{5}{2}\ \frac{1}{3}$	$\frac{1}{2}\ \frac{5}{2}\ \frac{2}{3}$

LAUEGEN[12] revealed that there were at least two crystallites in this sample, offset in the *ab* plane by some angle which is a multiple of 60°. Each crystallite shares a common c^* axis, perpendicular to the plane of the crystal. The (0 0 1) reflection common to the crystallites is indicated in Fig. 2. The lamellar appearance of both the crystal and the unusually broad nuclear reflections suggests that the sample consisted of many platy crystals, which share a nearly common c^* axis. The magnetic peaks are most obvious near the center of the 5 K pattern at low scattering angles where the magnetic form factor is largest. By trial and error the magnetic peaks could be indexed with a unit cell that was twice as large in *a* and *b* and around three times as large in *c*, which would correspond to propagation vectors of $\frac{1}{2}\ \frac{1}{2} \pm \frac{1}{3}$ in the conventional nuclear unit cell. According to this method of magnetic peak assignment, the two clearest magnetic peaks to the immediate left of the central position were labeled $(-\frac{1}{2}\ -\frac{1}{2}\ -\frac{1}{3})$ for the peak marked (1) and $(-\frac{1}{2}\ \frac{1}{2}\ -\frac{1}{3})$ for (2). The magnetic peaks were often assigned two sets of indices to describe the two most prominent crystallites in the sample. The classification of the principal magnetic reflections in Fig. 2 is listed in Table I. The indexing of the magnetic reflections is still uncertain due to their small number and diffuseness, and to a lesser extent to the radial projection in reciprocal space in the Laue technique.

The first scans at 20 K on D19 confirmed immediately that the propagation vector was very close to $[\frac{1}{2}\ \frac{1}{2}\ \frac{1}{3}]$. The intensities of the magnetic peaks were found to be maximum at positions where $l_{mag}=l_{nuc}\pm 0.34$; however, significant magnetic intensity was also found up to ±0.15 reciprocal lattice units away from these positions along c^*. This indicates an elongation of the magnetic peaks into rodlike structures in reciprocal space, which is a sign of incomplete long-range order along the *z* direction. A magnetic sample with long-range three-dimensional (3D) order would have an intensity profile with very sharp peaks at the reciprocal lattice positions in the magnetic unit cell. The elongation of the magnetic reflections observed on D19 corresponds well with the streaky characteristics observed in the VIVALDI patterns as well as the breadth of the low-angle magnetic reflections in the powder diffraction pattern.[7]

The extension of the magnetic reflections along c^* led to partial overlap of the $(h+\frac{1}{2}\ k+\frac{1}{2}\ l+0.34)$ and $(h+\frac{1}{2}\ k+\frac{1}{2}\ l+0.66)$ reflections. To ensure full integration of the magnetic scattering, and to aid the extraction of individual magnetic intensities, the magnetic reflections were collected on D19 by extended scans along c^* centered at $(h+\frac{1}{2}\ k+\frac{1}{2}\ l+0.5)$ and over a sufficient range to scan through both the $l+0.34$ and $l+0.66$ reflections.

Because of the partial overlap of the $l+0.34$ and $l+0.66$ reflections in each scan, their integrated intensities were obtained by fitting two peaks to the projection of the 3D count distribution of the scan onto *l*, with the appropriate Lorentz correction applied to obtain the observed squared structure-factor amplitude.[14] In all these scans the profile of the magnetic reflections could be approximated very well by a Voigtian profile consisting of a Lorentzian convoluted with a considerably narrower Gaussian. The Gaussian profile was chosen to match the instrumental resolution function of D19 determined from nearby nuclear reflections. The half-widths of the Lorentzian profiles were constrained to be equal for all magnetic peaks in a given scan and the background was similarly constrained to be flat. The intensity profile along $(\frac{3}{2}\ \frac{1}{2}\ l)$ for crystallite B can be seen in Fig. 3, where the continuous line represents the best fit to the data. Fitting the scan through the $(\frac{3}{2}\ \frac{1}{2}\ 0.34)$ and $(\frac{3}{2}\ \frac{1}{2}\ 0.66)$ reflections to a pair of Lorentzians convoluted with the Gaussian gave a mean Lorentzian full width at half height of 0.11 (±0.02) in *l*.

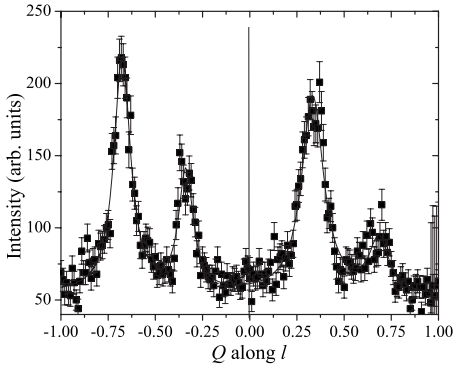

FIG. 3. Intensity profile along the reciprocal lattice vector, $(\frac{3}{2}\ \frac{1}{2}\ l)$, for crystallite B. The curve represents the fit of four Voigtian profiles to the observed data.

Due to time constraints, only a limited number of magnetic reflections could be scanned. A list of the most intense magnetic peaks observed on D19 for each crystallite is given in Table II.

The thermal variation of the reduced magnetic moment was also observed from the integrated D19 data. A plot of the integrated magnetic intensity of the $(\frac{3}{2}\ \frac{1}{2}\ 0.66)$ as a function of temperature can be seen in Fig. 4. The magnetic intensity remains at a constant maximum value for temperatures below 100 K, and decreases sharply above 100 K to reach zero at the Néel temperature of 117 K. This squarelike profile is an indication of the strong anisotropy of $FePS_3$ as well as of possible 2D magnetic ordering. The fits included in Fig. 4 shall be discussed in Sec. IV B.

IV. DISCUSSION

In deriving possible magnetic structures, constraints from the results of other experimental techniques were considered. From transmission, single-crystal Mössbauer spectroscopy experiments, with the γ-ray direction perpendicular to the *ab* plane, four absorption lines were observed in the magnetically ordered spectrum.[15] The absence of lines 2 and 5 from a typical six-line spectrum indicated that the moments are

TABLE II. The most intense magnetic peaks observed with D19 were assigned to either one or both of the twinned magnetic crystallites.

Crystallite A		Crystallite B	
hkl	Intensity (arb. units)	*hkl*	Intensity (arb. units)
$\bar{\frac{3}{2}}\ \bar{\frac{7}{2}}\ 0.34$	26±1	$\frac{1}{2}\ \bar{\frac{1}{2}}\ \overline{0.66}$	45.5±0.5
$\frac{1}{2}\ \bar{\frac{1}{2}}\ \overline{0.66}$	25.1±0.3	$\frac{3}{2}\ \bar{\frac{1}{2}}\ \overline{0.66}$	30.7±0.7
$\frac{1}{2}\ \frac{11}{2}\ \overline{0.66}$	23±1	$\frac{3}{2}\ \frac{1}{2}\ \overline{1.34}$	28.9±0.7
$\frac{1}{2}\ \bar{\frac{1}{2}}\ 0.34$	18.6±0.4	$\frac{1}{2}\ \frac{1}{2}\ \overline{0.66}$	24.9±0.3
$\frac{1}{2}\ \frac{11}{2}\ 0.34$	18±1	$\frac{3}{2}\ \frac{1}{2}\ \overline{0.34}$	13.5±0.6
$\bar{\frac{1}{2}}\ \bar{\frac{5}{2}}\ 0.34$	16.1±0.8	$\frac{5}{2}\ \bar{\frac{1}{2}}\ \overline{0.66}$	9.9±0.9
$\frac{1}{2}\ \bar{\frac{7}{2}}\ \overline{0.34}$	11±1	$\frac{5}{2}\ \bar{\frac{1}{2}}\ \overline{1.66}$	9±1
$\frac{1}{2}\ \bar{\frac{3}{2}}\ \overline{0.34}$	6.8±0.5	$\frac{5}{2}\ \frac{1}{2}\ \overline{0.66}$	8.5±0.9

directed perpendicular to the *ab* plane. Magnetic susceptibility measurements have been taken at temperatures close to absolute zero for applied fields both parallel and perpendicular to the trigonal axis, that is, the *z* direction.[16] These measurements indicated that the susceptibility dropped to around zero for fields applied parallel to *z*. Both sets of results support a magnetic structure where the moments are oriented along the *z* direction, perpendicular to the *ab* plane.

The magnetic interactions in $FePS_3$ and $MnPS_3$ were initially considered to be similar, both with strong intraplanar interactions and weak interplanar interactions. Incomplete long-range order is not uncommon in the thiophosphate materials, with $MnPS_3$ showing evidence of short-range magnetic correlations in powder neutron diffraction patterns.[17] However, a single-crystal study of $MnPS_3$ by Wildes *et al.*[18] shows that the rodlike features observed at 100 K, above T_N, and attributed to critical scattering are virtually absent at 8 K indicating that the magnetic order is long ranged in all directions at low temperatures. Neglecting any microscopic differences that there might be between the powder and single-crystal materials, the trailing edges to the magnetic Bragg peaks observed in powder samples[17] must be due to something other than incomplete magnetic order, probably excitation of the low-lying magnon branch in $MnPS_3$ perpendicular to the planes. The magnetic ordering of $FePS_3$ is clearly rather different to that of $MnPS_3$.

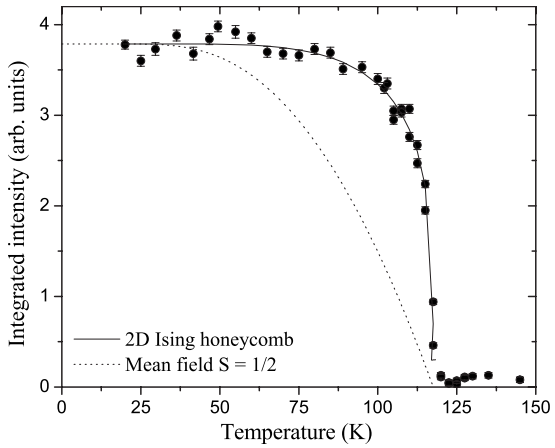

FIG. 4. The thermal variation of the integrated intensity of the $\frac{3}{2}\ \frac{1}{2}\ 0.34$ magnetic peak of $FePS_3$ recorded on D19.

A. In-plane structure

The structure within the *ab* plane was modeled by various sets of moments oriented parallel and antiparallel to the c^* direction. The in-plane structure of the moments was also constrained by the VIVALDI and D19 data, which indicated that the magnetic unit cell was twice the size of the nuclear unit cell in both the *a* and *b* directions. These models were first tested by least-squares fitting to the powder diffraction data taken at 5 K. Using the program FULLPROF,[19] the magnetic peaks over the scattering range of 0°–60° in 2θ were fitted using the original in-plane structure proposed by Le Flem *et al.*[6] [Fig. 1(b)]. Due to a number of factors including preferred orientation within the powdered sample and fitting the peaks with a sharp peak shape, a perfect fit was not obtained. Another consideration for the in-plane moment structure involved the propagation vectors associated with each model. The original in-plane model proposed by Le Flem *et al.* was found to describe the configuration of the moments best as it was the only structure with just one set of propagation vectors, $\left[\frac{1}{2}\ \frac{1}{2}\ l\right]$ and $\left[-\frac{1}{2}\ -\frac{1}{2}\ l\right]$ with equivalent *d* spacings. The magnetic peaks in the powder pattern occur at scattering angles that follow this propagation vector only; thus, although other structures had the correct dimensions, only this structure had both the correct dimensions and in-plane propagation vector. The exchange field in $FePS_3$ was also calculated to be 32 T from this in-plane moment structure, which corresponds within error to the exchange field observed in high-field magnetization measurements.[20]

B. Magnetic order along the c^* direction

The magnetic structures of other members of the thiophosphate family, and even the $MPSe_3$ family (where *M* =transition metal), are well documented and known to be 3D.[21,22] However, the exchange interactions between the planes of metal ions are often much weaker than between metal atoms within the plane—up to 400 times less for $MnPS_3$.[22] Incomplete long-range order in $MnPS_3$ was evident as trailing edges on the high-scattering side of the magnetic peaks in the powder neutron diffraction pattern.[17] A similar feature observed in the $FePS_3$ powder diffraction pattern was a broad, yet low-intensity hump on the high-scattering side of the sharp magnetic peaks as seen in the upper panel of Fig. 5. These humps could be Bragg reflections, but they may also be an indication of incomplete long-range order.

From the D19 data, the streakiness was initially attributed to weak correlations between interplanar Fe^{2+} ions. However, neither a commensurate magnetic structure with a wave vector of $\left[\frac{1}{2}\ \frac{1}{2}\ \frac{1}{3}\right]$ nor an incommensurate magnetic structure with a wave vector of $\left[\frac{1}{2}\ \frac{1}{2}\ 0.34\right]$ could describe the streaki-

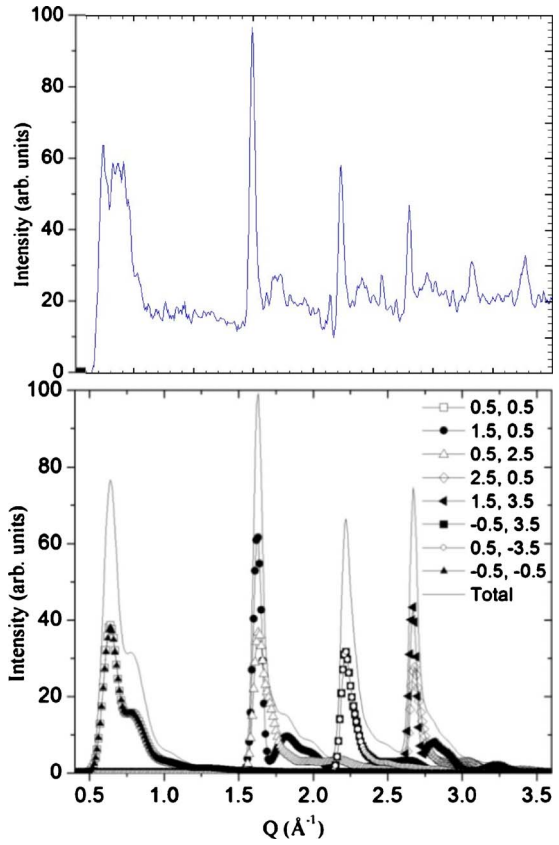

FIG. 5. (Color online) Upper panel: the MRPD powder diffraction pattern where the nuclear peaks have been subtracted such that only magnetic peaks remain. Lower panel: simulation of the magnetic peaks with propagation vectors of $\left[\frac{1}{2}\ \frac{1}{2}\ l\right]$ and $\left[-\frac{1}{2}\ -\frac{1}{2}\ l\right]$ associated with the (0 0 0), (1 3 0), and (2 0 0) nuclear reflections. This simulation includes all magnetic peaks below $Q=2.9$ Å^{-1}.

ness of the peaks along l as both structures would give well-defined spots in the Laue scan if any long-range order were present. Instead the elongated peaks were caused by short-range correlations between metal atoms along the crystallographic z direction. From this, a simulation was produced to describe the expected powder diffraction pattern for the magnetic peaks as seen in the lower panel of Fig. 5. The first two major magnetic peaks were approximated with a Gausssian line shape. These peaks were found according to the propagation vector that best fit the in-plane structure above. This was the pair of vectors $\left[\frac{1}{2}\ \frac{1}{2}\ l\right]$ and $\left[-\frac{1}{2}-\frac{1}{2}\ l\right]$ applied to the (0 0 0), (1 3 0), and (0 2 0) nuclear reflections. Thus the magnetic reflections were, respectively, the $\left(\frac{1}{2}\ \frac{1}{2}\ l\right)$ lines with a scattering angle of around 9.6° in 2θ and the $\left(\frac{1}{2}\ \frac{5}{2}\ l\right)$ and $\left(\frac{3}{2}\ \frac{1}{2}\ l\right)$ lines centered around 25° in 2θ. Each peak was created from the sum of peaks with $l=\pm 0.34$, ± 0.66, ± 1.34, ± 1.66. The peak intensity of the simulation was also adjusted by including a magnetic form factor in the calculations. A Gaussian function for metallic iron was used to approximate the form factor using the data obtained by Shull and Yamada as illustrated in Ref. 23.

From the D19 profiles, the thermal variation of the short-range order was examined in terms of the change in the sublattice moment and magnetic periodicity. The peak positions did not deviate from their initial values of 0.34 and 0.66 for all temperatures below the Néel temperature indicating that the ordered magnetic structure remains fixed at all temperatures. This would indicate that although there are only short-ranged correlations between the iron atoms along z, the structure does not appear to relax into some long-ranged 3D order. Above the Néel temperature, weak intensities were still present at 0.34 and 0.66 suggesting the presence of critical scattering similar to that observed in $MnPS_3$.[24]

Powder diffraction patterns for magnetic structures with the in-plane models proposed by Le Flem *et al.*[6] and Kurosawa *et al.*[8] are very similar, due to the nearly regular hexagonal arrangement of the Fe atoms in the *ab* plane. This would also be true for the 2D-averaged data that were observed by Kurosawa *et al.*, and explains why their data could be modeled by a propagation vector of [0 0] in the *ab* plane. The nearly regular hexagonal Fe arrangement also explains the twinning of the crystals.

To confirm the 2D nature of the magnetic ordering, the thermal variation of the sublattice moment (Fig. 4) was fitted with the honeycomb-lattice 2D Ising model.[25] This model assumes only first-neighbor antiferromagnetic interactions so that the resulting 2D order would be the same as for $MnPS_3$ and not the same as for this material. Nevertheless it is the closest solved model to our system. Additionally the Ising model for any 2D lattice results in the same precipitous decline in sublattice moment as observed in our data, quite different from the $S=\frac{1}{2}$ mean-field model which does not depend on dimensionality. The expression for the model is

$$M = \left[1 - \frac{16z^3(1+z^3)(1+z^2)^3}{(1-z^2)^6}\right]^{1/8}, \qquad (1)$$

where $z=\exp(-2K)$ and $K=\frac{J}{k_BT}$.

The fit gave $T_N=117.52$ K and $J=70.89$ K. In assessing this J it must be remembered that it refers to a situation in which there are first-neighbor interactions only.

As can be seen, the mean-field model does not appear to represent the data well at temperatures between 80 and 120 K, while the 2D Ising lattice shows a remarkable resemblance to the D19 results. Thus, of the two models, the 2D Ising honeycomb lattice better describes the temperature variation of the reduced magnetic moment. Neutron diffraction studies by Wiedenmann *et al.*[21] and Kurosawa *et al.*[8] have both shown evidence of a 2D in-plane structure in the MPX_3 compounds (M=Mn and Fe, X=S and Se); however, neither has commented on the significance of their results. Each study displayed plots of the temperature dependence of the reduced magnetic moments, superimposed with a modeled 3D Brillouin function for different spin values $\left(S=\frac{1}{2},\frac{5}{2}\right)$. The data for the Mn compounds fitted the Brillouin curve of $S=\frac{5}{2}$ very well, as expected for a material with very little single-ion anisotropy and 3D order. The reduced magnetic moment of the Fe compounds appeared to remain constant for temperatures up to T/T_N 0.7, beyond which the magnitude of the moment fell sharply as T approached T_N. This sharp decrease is similar to that in Fig. 5 and can be attributed to the strong anisotropy of the Ising-type system and the 2D nature of the interactions.

From the current data, it appears as though the magnetic long-range structure of $FePS_3$ is truly 2D. Analysis of these data has shown that it is well modeled as a 2D Ising antiferromagnet. There are two other simple materials which appear to fit this description: Rb_2CoF_4 and K_2CoF_4. Both neutron diffraction results and susceptibility measurements of these two compounds showed similar features, which indicated that the magnetic dimensionality was similar in each case.[26,27] The rodlike scattering profiles in reciprocal space were a strong indication of incomplete long-range order, while the temperature dependent sublattice moment closely resembled the 2D Ising model. The dependence close to the critical temperature showed the typical $\frac{1}{8}$ Ising power law with the appropriate square-lattice prefactor for Rb_2CoF_4.

The widths of the peaks along the z direction for Rb_2CoF_4 were also sensitive to heat treatment raising the possibility that the short-range order might be metastable, even suggesting that the stable magnetic order is long range in all directions. Further work needs to be done to establish how true this is for $FePS_3$ but it should be mentioned that even if the short-range order is metastable the stable state might not be ordered at long range. If the strongly anisotropic planes are regarded as weakly coupled Ising objects this linear array would not order at any temperature.[28]

V. CONCLUSIONS

Laue neutron diffraction patterns have shown the magnetic reflections in $FePS_3$ to be streaky, indicating a lack of long-ranged magnetic order along the c^* direction. This was confirmed by single-crystal neutron diffraction scans on the monochromatic four-circle diffractometer, D19. This implies that the interactions between Fe ions along the c direction are very weak compared with the interactions within the ab plane. It also suggests a strong anisotropy in the magnetic structure. Similar materials with relatively little anisotropy, such as Rb_2FeF_4, have been observed to order in three dimensions. Fitting a monoclinic structure to the VIVALDI results also revealed a magnetic unit cell that was double the nuclear unit cell along both the a and b directions. Thus the set of propagation vectors to describe the magnetic reflections is $\left[\frac{1}{2}\ \frac{1}{2}\ 0.34\right]$ and $\left[-\frac{1}{2}\ -\frac{1}{2}\ 0.34\right]$. Peaks following this pattern corresponded well with the previous powder diffraction patterns.

The intensity profile of the magnetic peaks along the c^* direction corresponded to the modeled prediction that the order along l is indeed short ranged. The weak interlayer correlations between the moments were also responsible for the diffuse humps on the high-scattering angle side of the magnetic Bragg peaks observed in the powder diffraction pattern. Thus all the neutron diffraction results exhibit evidence of incomplete long-range magnetic order along the z axis in $FePS_3$.

The true magnetic order for $FePS_3$ was the same in the ab plane as that proposed by Le Flem *et al.*,[6] with ferromagnetic chains coupled antiferromagnetically. Between the layers long-range order is not well established, giving rise to a short-range ordering of moments along c even at low temperatures. Thus the propagation vector for $FePS_3$ is $\left[\frac{1}{2}\ \frac{1}{2}\ l\right]$ in the plane with an ill-defined l component of about 0.34 out of the plane.

Our results illustrate the strength of single-crystal diffraction to resolve ambiguities in magnetic structures, even those as simple as $FePS_3$, and the unique capability of Laue diffraction to locate magnetic reflections.

ACKNOWLEDGMENTS

This work was supported by the Australian Research Council. K.C.R. was the recipient of an Australian Postgraduate Award with a supplement from the Australian Institute of Nuclear Science and Engineering.

*kirrilyr@gmail.com

[1] W. Klingen, G. Eulenberger, and H. Hahn, Naturwiss. **55**, 229 (1968).
[2] P. A. Joy and S. Vasudevan, Phys. Rev. B **46**, 5425 (1992).
[3] F. S. Khumalo and H. P. Hughes, Phys. Rev. B **23**, 5375 (1981).
[4] A. H. Thompson and M. S. Whittingham, Mater. Res. Bull. **12**, 741 (1977).
[5] C. Berthier, Y. Chabre, and M. Minier, Solid State Commun. **28**, 327 (1978).
[6] G. Le Flem, R. Brec, G. Ouvrard, A. Louisy, and P. Segransan, J. Phys. Chem. Solids **43**, 455 (1982).
[7] K. C. Rule, S. J. Kennedy, D. J. Goossens, A. M. Mulders, and T. J. Hicks, Appl. Phys. A: Mater. Sci. Process. **74**, S811 (2002).
[8] K. Kurosawa, S. Saito, and Y. Yamaguchi, J. Phys. Soc. Jpn. **52**, 3919 (1983).
[9] K. C. Rule, S. J. Kennedy, and T. J. Hicks, Physica B **335**, 6 (2003).
[10] C. Wilkinson, J. A. Cowan, D. A. A. Myles, F. Cipriani, and G. J. McIntyre, Neutron News **13**, 37 (2002).
[11] http://www.ill.fr/YellowBook/VIVALDI/
[12] J. W. Campbell, J. Appl. Crystallogr. **28**, 228 (1995).
[13] http://www.ill.fr/YellowBook/D19/
[14] G. J. McIntyre and R. F. D. Stansfield, Acta Crystallogr., Sect. A: Found. Crystallogr. **44**, 257 (1988).
[15] K. C. Rule, J. C. Cashion, A. M. Mulders, and T. J. Hicks, Hyperfine Interact. **141**, 219 (2002).
[16] P. Jernberg, S. Bjarman, and R. Wappling, J. Magn. Magn. Mater. **46**, 178 (1984).
[17] D. J. Goossens, A. J. Studer, S. J. Kennedy, and T. J. Hicks, J. Phys.: Condens. Matter **12**, 4233 (2000).
[18] A. R. Wildes, M. J. Harris, and K. W. Godfrey, J. Magn. Magn. Mater. **177-181**, 143 (1998).
[19] J. Rodriguez-Carvajal, *Short Reference Guide of the Program FullProf* (Laboratoire Leon Brillouin, Saclay, 1998).
[20] K. Okuda, K. Kurosawa, and S. Saito, in *High Field Magnetism*, edited by M. Date (North-Holland, Amsterdam, 1983), pp. 55–58.
[21] A. Wiedenmann, J. Rossat-Mignod, A. Louisy, R. Brec, and J.

Rouxel, Solid State Commun. **40**, 1067 (1981).
[22] A. R. Wildes, B. Roessli, B. Lebech, and K. W. Godfrey, J. Phys.: Condens. Matter **10**, 6417 (1998).
[23] G. E. Bacon, *Neutron Diffraction*, 3rd ed. (Clarendon, Oxford, 1975).
[24] D. M. Burley, Philos. Mag. **5**, 909 (1960).
[25] R. J. Baxter, *Exactly Solved Models in Statistical Mechanics* (Academic, London, 1982).
[26] R. J. Birgeneau, H. J. Guggenheim, and T. N. Sairam, Phys. Rev. B **1**, 2211 (1970).
[27] E. J. Samuelsen, Phys. Rev. Lett. **31**, 936 (1973).
[28] E. Ising, Z. Phys. **24**, 253 (1925).